



WAGENINGEN
UNIVERSITY & RESEARCH

Population size mediates the contribution of high-rate and large-benefit mutations to parallel evolution

Nature Ecology & Evolution

Schenk, Martijn F.; Zwart, Mark P.; Hwang, Sungmin; Ruelens, Philip; Severing, Edouard et al

<https://doi.org/10.1038/s41559-022-01669-3>

This publication is made publicly available in the institutional repository of Wageningen University and Research, under the terms of article 25fa of the Dutch Copyright Act, also known as the Amendment Taverne. This has been done with explicit consent by the author.

Article 25fa states that the author of a short scientific work funded either wholly or partially by Dutch public funds is entitled to make that work publicly available for no consideration following a reasonable period of time after the work was first published, provided that clear reference is made to the source of the first publication of the work.

This publication is distributed under The Association of Universities in the Netherlands (VSNU) 'Article 25fa implementation' project. In this project research outputs of researchers employed by Dutch Universities that comply with the legal requirements of Article 25fa of the Dutch Copyright Act are distributed online and free of cost or other barriers in institutional repositories. Research outputs are distributed six months after their first online publication in the original published version and with proper attribution to the source of the original publication.

You are permitted to download and use the publication for personal purposes. All rights remain with the author(s) and / or copyright owner(s) of this work. Any use of the publication or parts of it other than authorised under article 25fa of the Dutch Copyright act is prohibited. Wageningen University & Research and the author(s) of this publication shall not be held responsible or liable for any damages resulting from your (re)use of this publication.

For questions regarding the public availability of this publication please contact openscience.library@wur.nl



Population size mediates the contribution of high-rate and large-benefit mutations to parallel evolution

Martijn F. Schenk^{1,2,7}, Mark P. Zwart^{1,3,4,7}✉, Sungmin Hwang^{3,5}, Philip Ruelens¹, Edouard Severing^{1,6}, Joachim Krug³ and J. Arjan G. M. de Visser¹✉

Mutations with large fitness benefits and mutations occurring at high rates may both cause parallel evolution, but their contribution is predicted to depend on population size. Moreover, high-rate and large-benefit mutations may have different long-term adaptive consequences. We show that small and 100-fold larger bacterial populations evolve resistance to a β -lactam antibiotic by using similar numbers, but different types of mutations. Small populations frequently substitute similar high-rate structural variants and loss-of-function point mutations, including the deletion of a low-activity β -lactamase, and evolve modest resistance levels. Large populations more often use low-rate, large-benefit point mutations affecting the same targets, including mutations activating the β -lactamase and other gain-of-function mutations, leading to much higher resistance levels. Our results demonstrate the separation by clonal interference of mutation classes with divergent adaptive consequences, causing a shift from high-rate to large-benefit mutations with increases in population size.

Public health threats from rapidly evolving pathogens, together with observations of convergent and parallel evolution, have stimulated recent efforts to explore the predictability of evolutionary processes^{1–5}. Yet, even our understanding of the contribution of fundamental mechanisms, such as mutation and selection, to parallel evolution in laboratory evolution experiments with asexual microbes is incomplete^{6–8}.

Mutations occur in various forms, with widely diverging rates and fitness effects. For example, gene duplications and deletions may occur at much higher rates than point mutations⁹ and fitness effects of beneficial mutations are broadly distributed, often with an exponential tail^{10–12}. These differences in rate and fitness effects of different mutations make their contribution to evolution conditional on population size^{13–15}. In sufficiently small populations (the so-called strong selection, weak mutation regime), high-rate and large-benefit mutations are predicted to impact adaptation similarly^{15,16}. In contrast, in large populations where multiple beneficial mutations are present simultaneously, selection dominates mutation choices, because clonal interference filters out small-effect mutations even when they have high rates^{17,18} (Supplementary Information; Fig. 1 and Supplementary Fig. 1). To what extent high-rate mutations also impact adaptation in large populations is the topic of current debate, based on theoretical arguments and observations of substitution biases among point mutations in genomic data and evolution experiments^{19–25}. Moreover, the net effect of population size on parallel evolution is non-trivial and depends on the actual rates and fitness effects of mutations and their variance and covariance^{15,19}, as well as on their epistatic interactions^{26–29}.

Given the predicted profound role of population size in determining mutation trajectories, recent studies have addressed its role by varying population bottlenecks in short-term evolution experi-

ments of antibiotic resistance^{14,30,31}. These studies revealed effects of different bottlenecks on the types of substitutions, but did not quantify the effects of clonal interference and mutation bias on parallel evolution. Also, little is known about the consequences of high-rate and large-benefit mutations for longer-term adaptation. For example, if high-rate mutations typically confer small fitness benefits, they may enhance evolvability by avoiding adaptive constraints in rugged fitness landscapes^{26,28,29,32}. Alternatively, if high-rate mutations inactivate genes that may contribute to adaptation via lower-rate mutations, their effect on evolvability may be negative³³. Here we investigate the effect of population size on the type, repeatability and adaptive consequences of substitutions in bacterial populations adapting to gradually increasing antibiotic concentrations. Our specific aim is to quantify the relative contribution of the rates and fitness effects of general mutation classes, such as point mutations, indels and structural variants, to the pattern of parallel evolution in populations of different size.

Results

Experimental evolution of cefotaxime resistance. Seventy-two small ($N_e \sim 2 \times 10^6$) and 24 large populations ($N_e \sim 2 \times 10^8$) of an *Escherichia coli* strain harbouring a multicopy non-conjugative plasmid expressing TEM-1 β -lactamase, evolved via serial transfer in Luria broth containing cefotaxime (CTX) (and tetracycline to avoid plasmid loss). These population sizes were chosen to differ in the expected intensity of clonal interference, on the basis of previous work with the same bacterial strain in the absence of antibiotics^{34,35}. The β -lactamase has very low activity against CTX, but can be activated by many different point mutations³⁶. To maintain a constant selection pressure that is comparable in small and large populations, CTX concentrations were increased by a factor

¹Laboratory of Genetics, Wageningen University and Research, Wageningen, the Netherlands. ²Wageningen Food Safety Research, Wageningen, the Netherlands. ³Institute for Biological Physics, University of Cologne, Cologne, Germany. ⁴Netherlands Institute of Ecology, Wageningen, the Netherlands. ⁵Present address: Capital Fund Management, Paris, France. ⁶Max Planck Institute for Plant Breeding Research, Cologne, Germany. ⁷These authors contributed equally: Martijn F. Schenk, Mark P. Zwart. ✉e-mail: M.Zwart@nioo.knaw.nl; arjan.devisser@wur.nl

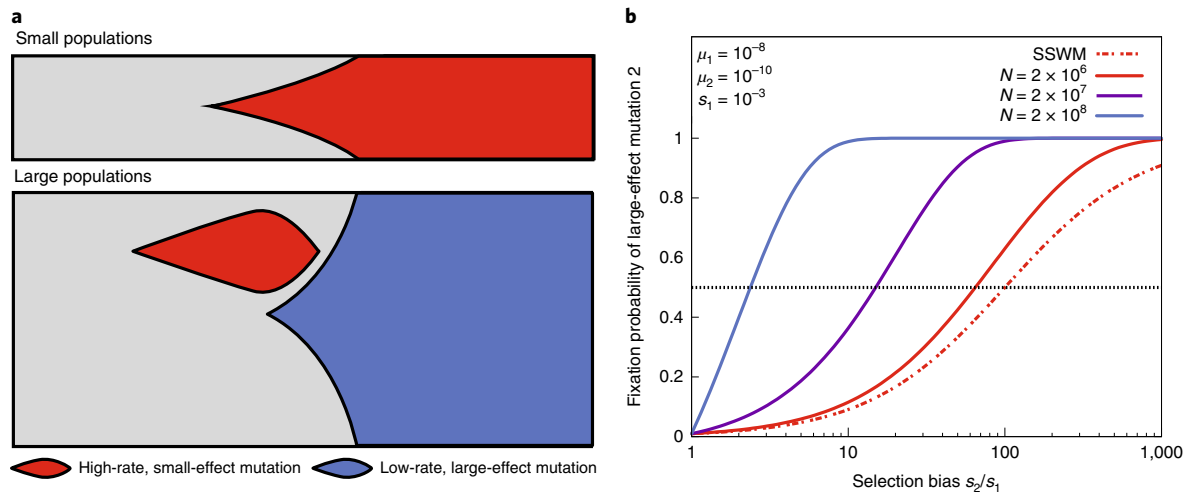


Fig. 1 | Expected relative impact of high-rate and large-benefit mutations in asexual populations of different size. a, In large populations, small-effect beneficial mutations (red) are filtered out due to clonal interference with large-effect mutations (blue), whereas the absence of the latter in small populations causes the high-rate mutations to dominate. The separation of high-rate and large-benefit mutations in populations of different size is facilitated when mutation rates and effects correlate negatively. **b**, Effect of population size on the relative fixation probability of two mutations, one (mutation 1) with a high rate ($\mu_1 = 10^{-8}$) and a small selective benefit ($s_1 = 0.001$), and another (mutation 2) with 100-fold lower rate, but up to a 1,000-fold larger benefit (equation 3 in Supplementary Information). While in small populations lacking clonal interference (SSWM, strong selection weak mutation) the relative benefit of mutation 2 should be equal to the inverse of its relative mutation rate to have equal fixation probability as high-rate mutation 1, in populations of the size of our large bacterial populations ($\sim 2 \times 10^8$), a two-fold benefit is sufficient.

of $2^{0.25}$ whenever the optical density of a population before transfer had risen above 75% of that in the absence of CTX, resulting in a 4.6-fold higher geometric mean CTX concentration in large than in small populations (Extended Data Fig. 1). Sixteen large control populations were evolved without antibiotics or with only tetracycline (Supplementary Table 2). After 50 transfers (~ 500 generations), a random clone was isolated from each population to determine the extent and repeatability of adaptation. Large populations showed markedly higher resistance levels than small populations (on average 12.8 versus 7.2 doublings of the minimal inhibitory concentration (MIC) of CTX, respectively; $U = 56.5$, $N = 96$, $P < 0.001$; Fig. 2a).

Differences in mutation numbers and types. Resequencing of the ancestral strains and 112 evolved clones revealed 1,190 mutations (Fig. 2b,c, and Supplementary Fig. 4 and Tables 5 and 6). These include 706 single-nucleotide polymorphisms (SNPs), 275 indels (< 1 kbp) and insertion-sequence (IS) element transpositions, 160 large deletions (> 1 kbp), 49 large duplications (> 1 kbp) and four 304bp inversions. Two clones from the small and three from the large CTX-treated populations were identified as mutators (Supplementary Information and Extended Data Fig. 2). Non-mutator CTX-treated clones had on average 9.5 mutations in small and 10.2 mutations in large populations ($U = 823$, $N = 107$, $P = 0.405$); clones from control populations had fewer mutations ($U = 1,352.5$, $N = 107$, $P < 0.0001$; 5.9 in the no-antibiotic and 6.0 in the tetracycline-only populations; Supplementary Figs. 6 and 7, and Extended Data Fig. 3). Among non-mutator clones, those from small populations showed fewer SNPs ($U = 1,186.5$, $N = 91$, $P < 0.0001$), particularly in their plasmid, while those from large populations had fewer structural variants (SVs, that is, deletions and duplications > 1 kbp; $U = 1,196$, $N = 91$, $P < 0.0001$) in both chromosome and plasmid (Fig. 2b; see Supplementary Table 1 for additional statistical comparisons in mutation numbers). Of the 503 SNPs observed in CTX-treated non-mutators, 14 were synonymous and 30 were intergenic. The normalized ratio of their non-synonymous

to synonymous substitutions per site (dN/dS: 11.9 in small, 28.8 in large populations; Supplementary Table 7) confirmed a dominant role for selection, with 92% and 97% of the non-synonymous substitutions expected to be beneficial in small and large populations, respectively.

Parallel mutations. To measure mutational repeatability, the average pairwise similarity of genotypes was calculated for non-mutator clones, by considering mutual overlap across all types of mutations (Supplementary Information and Supplementary Fig. 9). Consistent with previous findings^{8,37}, mutational repeatability was higher at the gene than at the nucleotide level ($U = 10,828$, $N = 107$, $P < 0.0001$; 34% versus 11% shared mutations, respectively; Fig. 3a). Repeatability was also higher in large than in small populations at the gene ($U = 149$, $N = 91$, $P < 0.0001$) and nucleotide levels ($U = 507$, $N = 91$, $P = 0.032$; Fig. 3a). However, SNPs and SVs contributed to this overall pattern of repeatability in opposite ways: clones from small populations consistently shared fewer SNPs but more SVs than clones from large populations, both at the nucleotide (Fig. 3b) and gene levels (Extended Data Fig. 4), in the chromosome as well as in the plasmid ($P < 0.001$ in all cases; see Supplementary Table 1 for additional statistical comparisons and Supplementary Tables 8 and 9 for repeatability results). What caused this greater repeatability of SNPs in large and SVs in small populations? We hypothesized that a combination of stronger clonal interference in large populations and a trade-off between rates and fitness effects of SNPs and SVs underlies their different contribution in small and large populations. If SNPs have both lower rates and larger benefits than SVs, clonal interference and stronger purifying selection would more often prevent high-rate SVs from fixing in large than in small populations.

Mutation supplies versus selective conditions. To maintain a constant selection pressure across populations, we adapted CTX concentrations to match the speed of adaptation of individual populations. Nevertheless, some large populations adapted as fast as

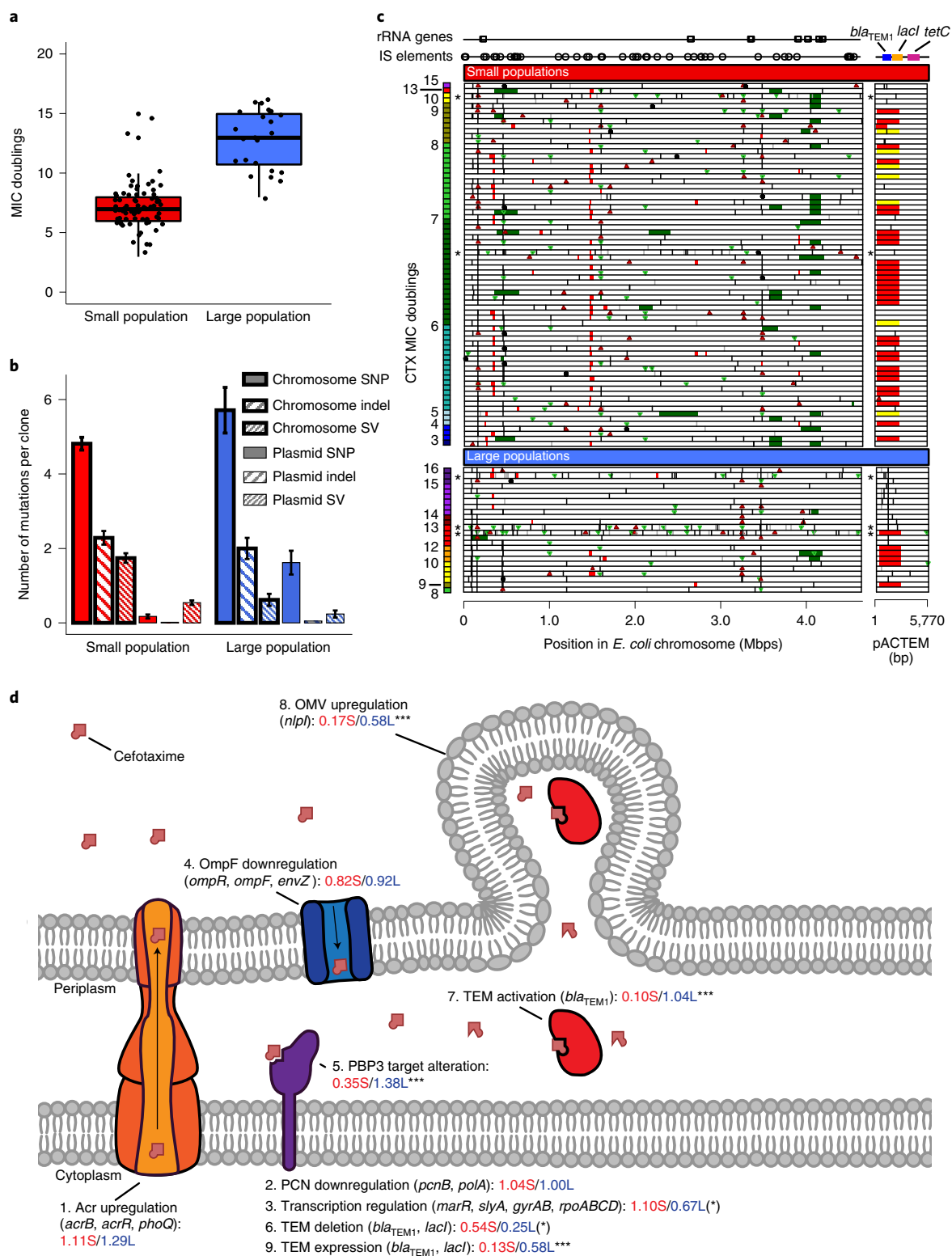


Fig. 2 | Phenotypic and genetic changes. **a**, Boxplots of the CTX MIC doublings of evolved clones from small (red) and large populations (blue) relative to the ancestral strain. Boxes show the median and interquartile range, and whiskers indicate the full range but exclude outliers. **b**, Number of mutations per category (means \pm s.e.m.), genomic element and population size for the 91 non-mutator clones. **c**, Position of mutations in chromosome and plasmid (different scales) for small (top) and large (bottom) populations ranked by their MIC value. Black vertical lines are SNPs, green and red triangles are small (<1kbp) insertions and deletions, respectively (indels), black circles are IS-element insertions, red and green bars are large (>1kbp) deletions and duplications, respectively (SVs, structural variants); yellow bars in the plasmid indicate heteroplasmic deletions; the five asterisks on the left indicate mutator genotypes; positions of IS elements and rRNA operons are indicated above. **d**, Functional targets with >20 mutations (Supplementary Information). Names of genes involved in each functional target are given between brackets, together with the average number of mutations per clone from small (red) and large (blue) populations. Asterisks show results from χ^2 tests of the difference in mutation frequencies in small and large populations: * $P < 0.10$, *** $P < 0.001$.

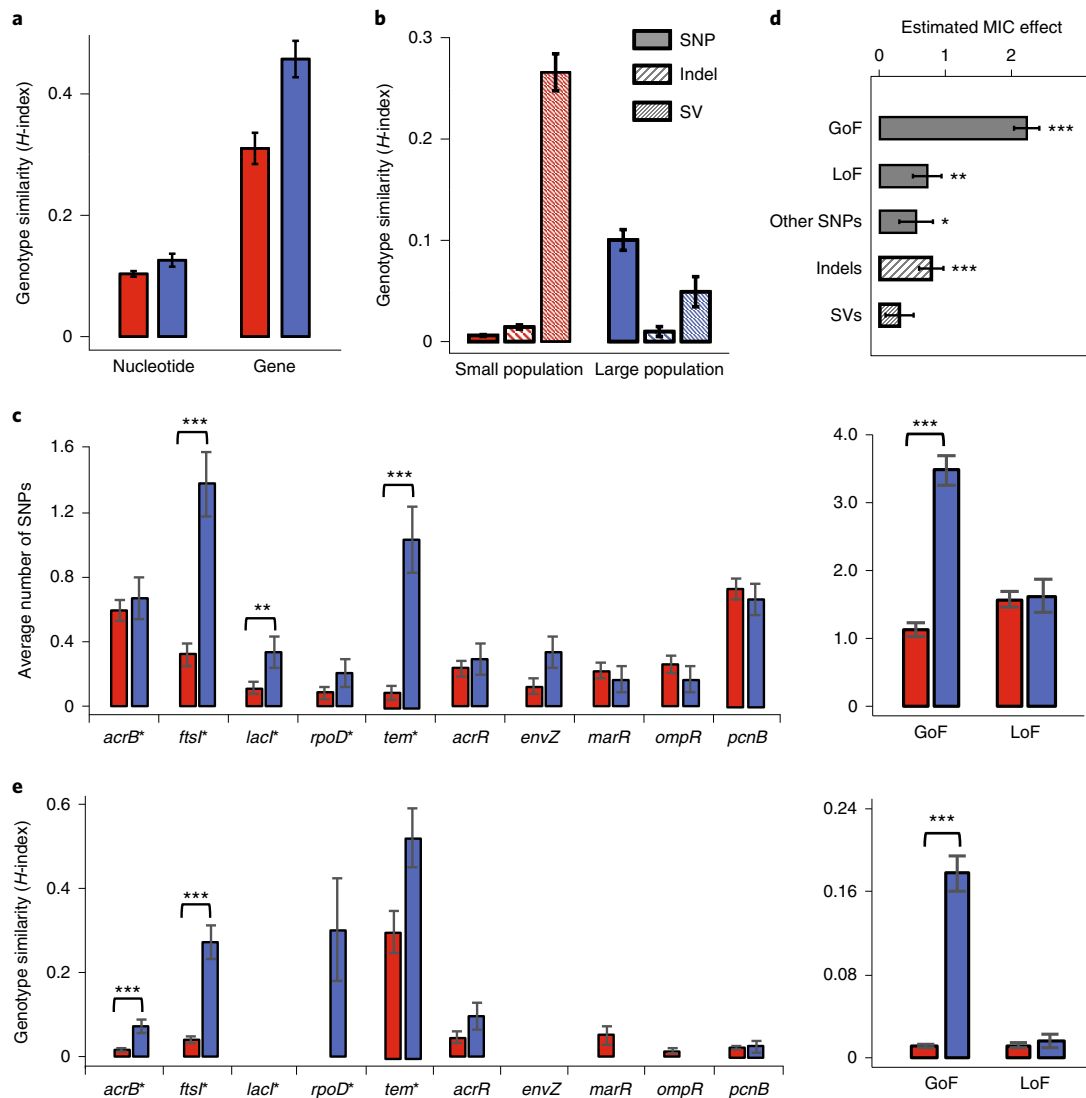


Fig. 3 | Repeatability of mutations and analysis of gain versus loss-of-function SNPs. a, Pairwise mutation similarity (means \pm s.e.m.) at the nucleotide and gene level for non-mutator clones, based on H -index (Supplementary Information). In this and the other panels, red refers to small populations, blue to large populations. **b**, Pairwise nucleotide-level mutation similarity per mutation class in chromosome and plasmid (means \pm s.e.m.). **c**, Frequency of SNPs in multiple-hit genes, categorized as GoF (indicated by asterisks) or LoF based on function and the presence/absence of inactivating mutations (Supplementary Information), shown for separate genes (left) and combined per category (right). Shown are mean frequency per clone (\pm s.e.m.). Asterisks above the columns indicate significant differences between small and large populations based on Mann-Whitney U tests; here and in **e**: * $P < 0.05$, ** $P < 0.01$, *** $P < 0.001$; *tem**, *bla*_{TEM1}. **d**, Estimates of the average effect (\pm s.e.m.) on CTX MIC of different mutation classes, using a general linear model (Supplementary Information). **e**, Nucleotide-level genotype similarity (mean H -index \pm s.e.m.) (left), categorized as GoF and LoF mutations (right) as shown in **c**.

or faster than CTX concentrations were increased (Extended Data Fig. 1), which may have introduced differences in selective conditions. We therefore first asked whether differences in selective conditions, rather than differences in mutation supplies, had an effect on the relative contributions of SVs and SNPs. Regression analysis showed no effect of variation in experienced CTX concentration on the fraction of SVs when tested for small and large populations separately ($P \geq 0.34$). Differences in experienced CTX concentration only affected the fraction of SVs for the combined populations ($P < 0.01$; Extended Data Fig. 5), indicating that primarily, differences in mutation supplies rather than CTX concentration per se, affected the contributions of the different mutation classes.

Were differences in selective conditions perhaps reflected by mutations in different targets in small and large populations? To examine this, we grouped all genes with ≥ 5 SNPs or indels across

all 96 populations into nine functional targets with ≥ 20 mutations (Supplementary Information and Table 14), which covered 57% of all mutations in these populations. The functional targets included known β -lactam resistance mechanisms, such as activation and upregulation of the AcrAB-TolC efflux pump, downregulation of outer-membrane porin OmpF, alteration of CTX-target PBP3 and activation of TEM-1 β -lactamase, but also unexpectedly the deletion of *bla*_{TEM1} and its repressor *lacI* from the plasmid (Fig. 2d). All nine targets were affected in small and large populations, albeit in subtly different ways: large populations more often activated the β -lactamase, altered target PBP3 and putatively increased the production of outer-membrane vesicles³⁸, while small populations tended to more frequently remove *bla*_{TEM1} and alter transcription regulation. Moreover, similar to the total set of mutations (Fig. 2b), these shared targets were also affected more often by SNPs in large

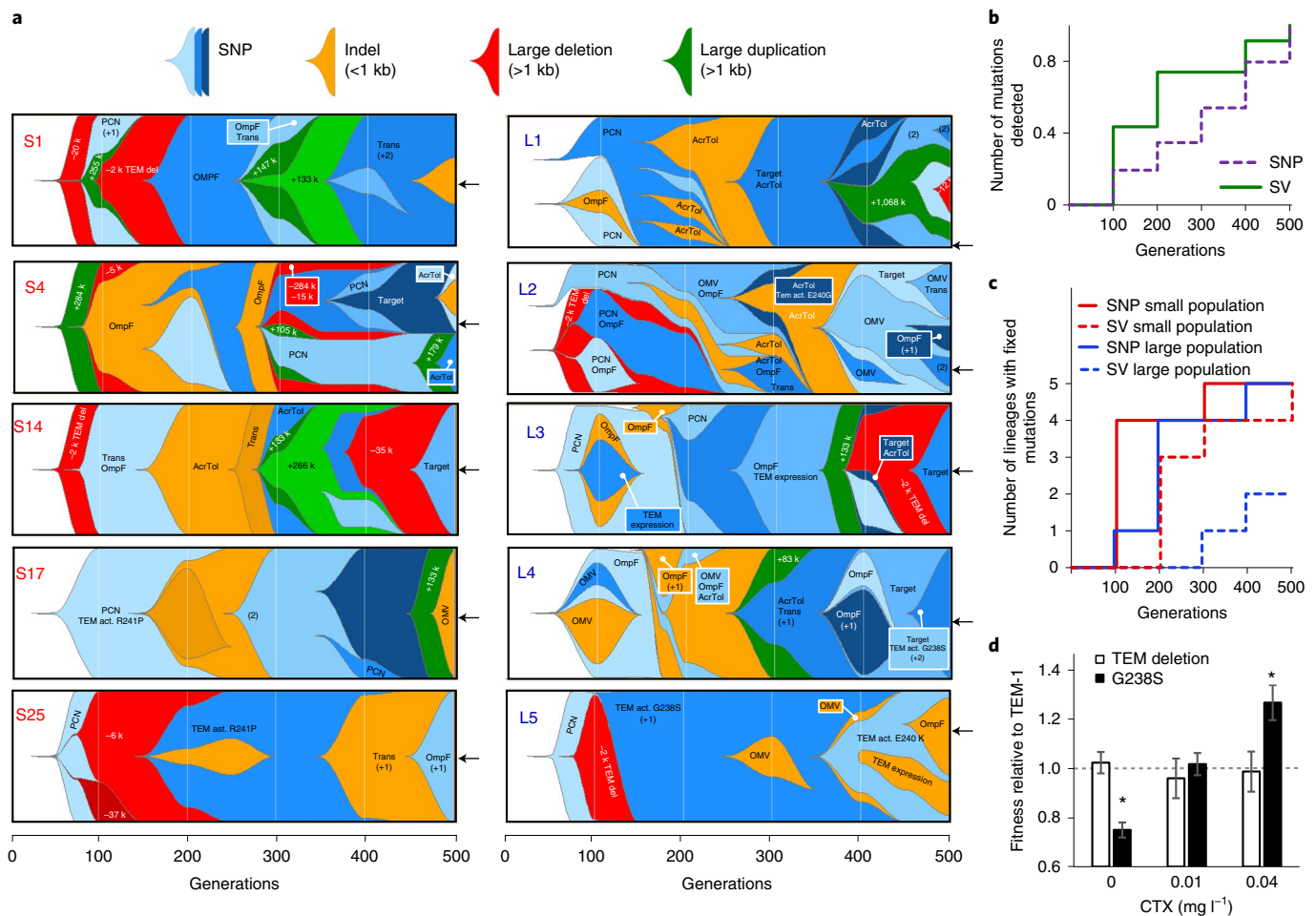


Fig. 4 | Temporal dynamics of genomic changes. **a**, Muller plots inferred for five small and five large populations on the basis of a comparison of population metagenomes at 100-generation intervals with final clone genotypes (indicated by black arrows). Shown are mutations reaching at least 10% frequency and the functional targets they affect (Fig. 2d), where applicable. **b**, Time to first detection of SNPs and SVs for the ten populations combined. **c**, Time to fixation of SNPs and SVs for small and large populations separately. **d**, Fitness effects of common ~2 kbp *bla*_{TEM}/*lacl* deletion and TEM-activating mutation G238S, measured in competition against the ancestral strain expressing TEM-1 in the absence and presence of CTX; **P* < 0.01 based on *t*-tests (see Supplementary Information for details).

populations and by SVs in small populations ($\chi^2 = 424.5$, $P < 0.0001$; Supplementary Table 14). Thus, small and large populations adapted via similar mechanisms, but differed in the frequency and types of mutations used, confirming that differences in mutation supplies rather than selective conditions drove these mutational differences.

Testing the clonal interference-trade-off hypothesis. To test our hypothesis that low-rate SNPs more often occur and survive clonal interference in large relative to small populations due to larger fitness benefits, we first examined differences in the temporal dynamics of mutations in small and large populations. For this, we sequenced the metagenomes of five small and five large populations at multiple time points. The inferred Muller plots (Fig. 4a) show stronger clonal interference in large populations, where the majority genotype detected at the initial time point never goes to fixation, while it fixes in all five small populations (Fisher's $P = 0.004$). The metagenomes also support the hypothesized differences in the rates and fitness effects of SNPs and SVs: SVs are detected earlier than SNPs (log rank test: $\chi^2 = 4.13$, $P = 0.042$; Fig. 4b) in both small and large populations, consistent with their expected higher rate³⁹, but in large populations fewer SVs fix than in small populations and they do so later than SNPs ($\chi^2 = 5.975$, $P = 0.015$; Fig. 4c), consistent with smaller fitness effects.

Second, we used Wright–Fisher simulations to estimate the average mutation rates and fitness effects of SNPs, indels and SVs that best explain their observed frequencies in the 91 non-mutator clones, assuming different exponentially distributed¹² and non-epistatic beneficial mutation effects for each class (Supplementary Information, Supplementary Table 11 and Extended Data Fig. 6). This yielded average selection coefficients of 0.41 for SNPs, 0.25 for indels and 0.14 for SVs, with corresponding mutation rates of 2.2×10^{-8} mutations per genome per generation for SNPs, 1.8×10^{-7} for indels and 7.1×10^{-6} for SVs, in support of our hypothesis. The relative selection coefficients of the three mutation classes were confirmed by estimating their effects on the measured MIC values of these clones using a general linear model, the estimated effects being approximately 2.5-fold larger for SNPs than for SVs (Supplementary Table 13).

Third, we sought to test whether the rate–benefit trade-off would also apply to other mutation classes than SNPs and SVs. Given the different frequencies of point mutations in small and large populations affecting certain functional targets (Fig. 2d), we wondered whether the more numerous mutations that inactivate a gene function (loss-of-function, LoF) would have smaller fitness effects than mutations that activate or subtly alter the function of a gene

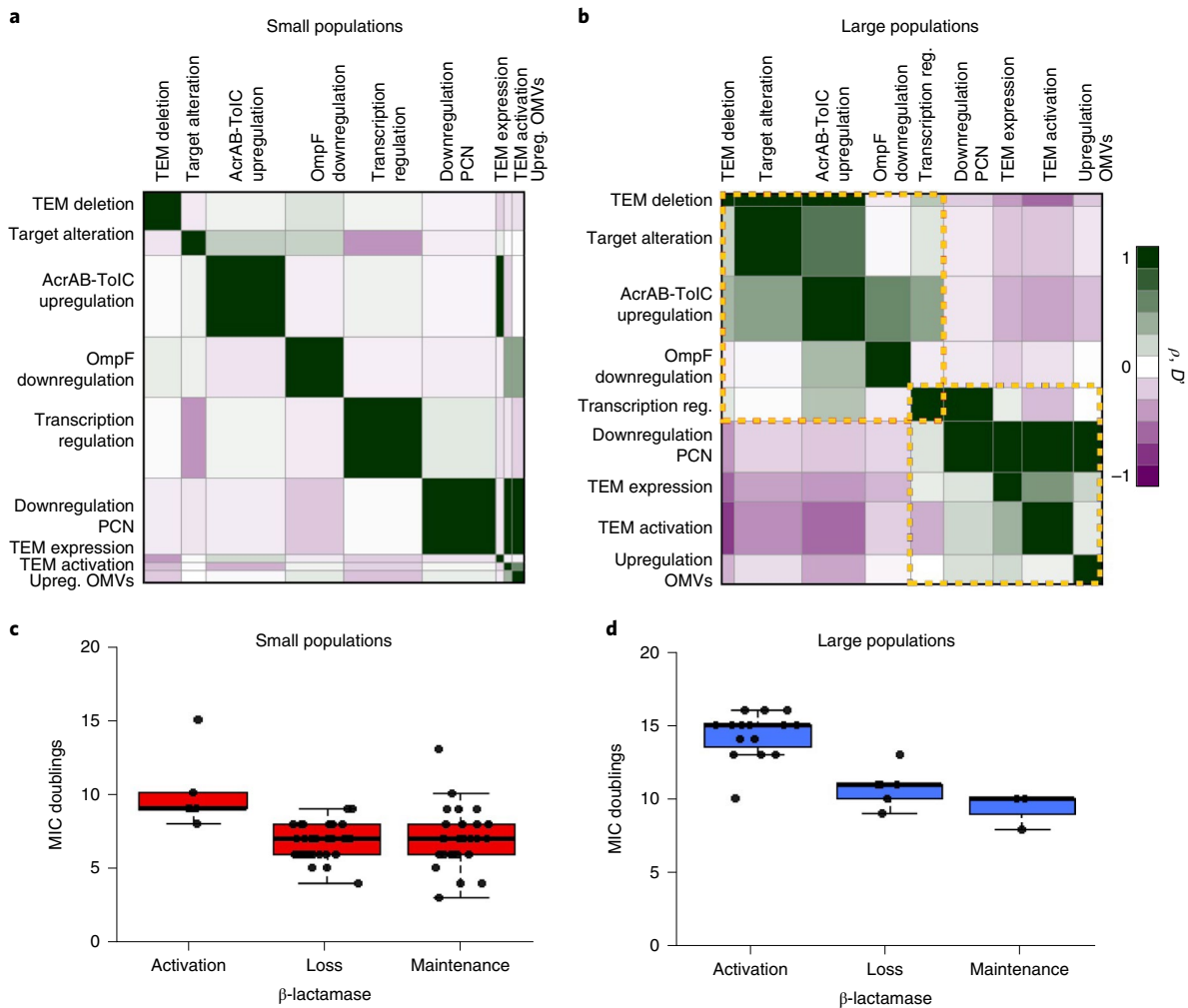


Fig. 5 | CTX resistance trajectories and their evolvability. a, b, Associations between functional targets with frequent mutations (Fig. 2d and Supplementary Table 14) in small (**a**) and large (**b**) populations, based on Spearman correlation (above diagonal) and normalized linkage disequilibrium⁵⁶ (below diagonal). Height and width of boxes reflect mutation frequencies, colours indicate negative (purple) to positive (green) associations. The yellow dashed boxes in **b** highlight two alternative trajectories involving the deletion or activation of TEM-1 β -lactamase. Upreg., upregulation; reg., regulation. **c, d**, MIC doublings of analysed evolved clones relative to the ancestral strain, for genotypes that activate, delete or maintain ancestral allele TEM-1, for small (**c**) and large (**d**) populations. Boxes show the median and interquartile range, and whiskers indicate the range but exclude outliers.

(gain-of-function, GoF), which have lower rates due to greater restrictions of the specific mutations required^{40,41}. To test whether GoF mutations have larger fitness effects than LoF mutations, we categorized genes with SNPs in multiple small and large populations (Supplementary Table 14) as putative GoF or LoF targets, on the basis of their function and the presence of indels or stop codons in at least two populations (Supplementary Information). Consistent with greater benefits of SNPs in GoF relative to LoF targets, the 174 SNPs in the five putative GoF targets (*bla*_{TEM1}, *fsl*, *acrB*, *lacl* and *rpoD*) occur more often in large than in small populations ($\chi^2 = 58$, $P < 0.0001$), while the 268 SNPs in the five putative LoF targets have comparable frequencies in small and large populations ($\chi^2 = 1.99$, $P = 0.158$; Fig. 3c). Also, estimates of the average MIC effects of putative GoF and LoF target SNPs using general linear models are approximately threefold higher for GoF than for LoF SNPs ($\chi^2 = 20.4$, $P < 0.0001$; Supplementary Information and Fig. 3d). This effect is partly, but not exclusively, driven by the large effects of SNPs activating the β -lactamase (GoF without TEM versus LoF, $\chi^2 = 6.2$, $P = 0.013$). Further, putative GoF mutations show greater repeatability in large than in small populations ($U = 62$, $N = 76$,

$P < 0.0001$; Fig. 3e), whereas putative LoF SNPs do not ($U = 251$, $N = 83$, $P = 0.215$). Therefore, a rate–benefit trade-off is supported for both the SNP/SV and GoF/LoF dichotomies, which suggests that this trade-off may be common or even ubiquitous. The sparsity of mutations with large benefits in empirical studies of the distribution of mutational effects^{11,42–44} further reinforces this suggestion.

Evolvability consequences of mutation choices. We finally examined the adaptive consequences of the different mutation choices of small and large populations. Following the approach of Tenailon et al.⁸, we first made an attempt to identify common mutation trajectories on the basis of associations between mutations in different functional targets (Supplementary Information). Clones from small populations showed no clear associations among mutated targets, whereas those from large populations revealed two alternative trajectories (Fig. 5b): one trajectory combining the deletion of *bla*_{TEM1} and *lacl* from the plasmid with alteration of CTX-target PBP3, the upregulation of efflux pump AcrAB-TolC and downregulation of OmpF, and another trajectory where TEM activation is associated with the regulation of its expression, downregulation of plas-

mid copy number and upregulation of outer-membrane vesicles. Importantly, populations activating TEM reach on average approximately 10-fold higher resistance levels than those deleting TEM ($U = 762.5$, $N = 56$, $P < 0.0001$; Fig. 5c,d), indicating significant differences in adaptive consequences.

Because the SV that removes TEM β -lactamase precludes its activation via SNPs, while the latter mutations may conversely prevent its subsequent loss, these two mutually exclusive mutations seem to drive the choice between the two alternative trajectories. Using pairwise competition assays (Supplementary Information), we found that the deletion of bla_{TEM} , which was twice as common in small than in large populations, was nearly neutral (Fig. 4d and Supplementary Information), indicating that it was driven by its high mutation rate alone. The high rate of this recombinational deletion was likely driven by two identical 184 bp sequences introduced during the construction of the plasmid (Supplementary Fig. 2). In contrast, activating SNP G238S, which has a much lower rate, had a fitness cost in the absence of CTX, but a substantial benefit under the selective conditions (Fig. 4d), explaining the higher frequency of large (63%) than small populations (8%) with TEM-activating mutations. An illustrative example of the sequential occurrence and competition between these mutations is population L5 (Fig. 4a), where a mutant with the bla_{TEM} deletion has seemingly fixed by 100 generations, but is subsequently driven extinct by a clone carrying TEM-activating mutation G238S (together with an SNP in *mraW*, encoding an S-adenosyl-methyltransferase).

Discussion

Several recent laboratory evolution studies have reported the substitution of mutations in different targets in bacterial populations experiencing different bottlenecks^{14,28,30,31,45,46}. We show that information about the average rates and fitness effects of common mutation classes may be sufficient for explaining the divergent mutation choices of different-sized populations. This implies that in our study, epistatic interactions were relatively weak, whereas in previous selection experiments where bla_{TEM1} was the only mutation target, epistatic constraints had a notable effect on the mutation trajectories of different-sized populations²⁸. Likely reasons for this difference are the availability of many more mutation targets and weaker epistasis among mutations in different genes reported here compared with mutations in a single gene (bla_{TEM1})¹. Still, the identification of two common mutation trajectories in the large populations suggests that epistasis may have also affected mutation choices in our present study. In fact, the mutual exclusion of TEM deletion and activation effectively also constitutes epistasis, constraining subsequent evolution in a similar way as the negative-sign epistatic interaction between two key activating mutations in bla_{TEM1} ²⁷. Therefore, including information about epistasis may improve predictions of mutational trajectories based on fitness models of individual resistance targets⁴⁷.

The observed trade-off between the rates and fitness effects of major mutation classes promotes divergent evolutionary fates of different-size populations, because it facilitates the separation of high-rate and large-benefit mutations by clonal interference. It is important to note that the rate–benefit trade-off we report involves substitutions rather than the full set of underlying mutations. Nevertheless, our data show that low-rate SNPs have a greater adaptive potential than high-rate SVs. This notion is supported by recent analyses of the long-term evolution experiment (LTEE) with the same *E. coli* strain in the absence of antibiotics, where the frequency of IS-related mutations, including many SVs⁴⁸, correlated negatively with fitness and was lower in populations showing point-mutation hypermutability, suggesting that point mutations provide greater benefits³³. Conceivably, fitness benefits of SVs are limited due to their larger off-target pleiotropic effects. However, it is unclear whether the larger fitness effects of SNPs that gain or subtly alter

a gene function (for example, to avoid antibiotic binding) relative to loss-of-function SNPs are also due to limited pleiotropy, and whether they hold beyond our study. Conserved genes that are part of *E. coli*'s core genome have been implicated as prominent targets for adaptive mutations in the LTEE⁴¹, as well as for antibiotic resistance⁴⁹. In our study, only two of the five putative gain-of-function targets (*ftsI* and *rpoD*) are part of *E. coli*'s core genome, highlighting an important role for accessory genes instead. A better understanding of the relationship between fitness effects and pleiotropic properties of mutations in these various targets may help to test the generality of our findings.

The most prominent high-rate mutations in our study were large chromosomal deletions, which are caused by intra-chromosomal recombination between repetitive sequences, such as IS elements. Consistent with previous findings³³, these high-rate mutations had a notable negative effect on evolvability, because they sometimes removed genes with longer-term adaptive potential, such as bla_{TEM1} . However, intra-chromosomal recombination may also cause similarly high-rate chromosomal duplications and gene amplifications, with potentially positive evolvability consequences due to enhanced survival under stress⁵⁰ and increased mutation supplies³⁹. Irrespective of the actual consequences, interactions between high-rate SVs and large-benefit SNPs are relevant for the evolution of antibiotic resistance, since antibiotic-resistance genes are often flanked by repeat sequences that facilitate their rapid deletion or amplification⁹.

Previous studies have addressed the effect of population size on the repeatability of evolutionary changes in experimental populations of asexual microbes, finding maximum repeatability in large^{13,14,28,35,51}, intermediate⁵² or small populations⁵³. Here we show that more intense clonal interference in large populations, together with knowledge of the variance and covariance of the rates and fitness effects of substitutions, may explain these divergent findings. Paradoxically, while in our system the negative covariance of rates and fitness effects among mutation classes reduces the positive effect of population size increase on repeatability, it also enhances the predictability of mutation choices of different-sized populations from information about the rates and fitness effects of common-target mutations. Our findings advocate a more prominent role of population size in efforts to predict evolution.

Methods

Media and bacterial strains. For all experiments, we used a modified Luria broth (LB), which here is 10 g l⁻¹ trypticase peptone, 5 g l⁻¹ yeast extract and 5 g l⁻¹ NaCl. For plates, 15 g l⁻¹ agar was added. *E. coli* strains REL606 (Ara-) and REL607 (Ara+)³⁴ were used for all experiments.

Evolution experiment. We electro-transformed REL606 and REL607 cells derived from a single colony with the pACTEM1 plasmid expressing TEM-1 β -lactamase⁵⁵ and subsequently plated them on LB supplemented with 15 μ g ml⁻¹ tetracycline for selection of transformants. A different colony was used to initiate 72 small, 24 large and 16 control populations (large populations with no antibiotics or tetracycline only, $N = 8$ each). Colonies were grown overnight in 1 ml LB with 15 μ g ml⁻¹ tetracycline. These overnight cultures were then used to initiate the serial passaging experiment with a 1:1,000 dilution in LB with different supplements depending on the treatment (Supplementary Table 2), including 0.011 μ g ml⁻¹ cefotaxime (CTX), 50 μ M isopropyl β -D-1-thiogalactopyranoside to induce TEM expression, and 15 μ g ml⁻¹ tetracycline to force plasmid maintenance (except for control populations C1–8). Small populations were represented by 200 μ l cultures in 300 μ l flat-bottom wells, distributed in a checkerboard pattern across two 96-well microtitre plates (ThermoFisher Nunc): Ara+ and Ara- populations were alternated and wells in between bacterial cultures were filled with sterile medium to control for potential contamination. Large populations were represented by 20 ml cultures in 50 ml tubes (Greiner) and were also transferred in alternating fashion with respect to Ara-marker. All cultures were kept at 37 °C with agitation (220 r.p.m.).

Transfers involved daily 1:1,000 dilutions (volume:volume) for 50 subsequent days (equivalent to ~500 bacterial generations). In the absence of CTX, these conditions yielded effective population sizes of $\sim 2 \times 10^6$ and $\sim 2 \times 10^8$ for small and large populations, respectively. These population sizes were chosen on the basis of the expectation of substantial differences in the strength of clonal interference

from previous work³⁴. To maximize selection for CTX resistance, we increased the concentration of CTX as follows. Before transfer, the optical density (OD₆₀₀) was measured with a Victor³ plate reader (Perkin Elmer). When the OD₆₀₀ was at least 75% of that of the ancestral strain in the absence of CTX, the concentration of CTX was increased by a factor of 2^{0.25} (~19%), so that after four increases the concentration doubled (Extended Data Fig. 1). In rare cases when the OD₆₀₀ dropped below 25% of its maximum, the concentration of CTX was decreased by a factor of 2^{0.25}. After 10, 20, 30, 40 and 50 transfers, samples were plated on TA agar to check for Ara-marker, and glycerol stocks of the populations were prepared and stored at -80°C.

Further methods and results. Additional methods, including for genomic and statistical analyses, and results are described in Supplementary Information.

Reporting Summary. Further information on research design is available in the Nature Research Reporting Summary linked to this article.

Data availability

There are no restrictions on data availability. Accession codes for reference sequences used are provided in Supplementary Information (REL606 genome: Genbank NC_012967.1; pACTEM1 plasmid: Genbank MN386081). Raw sequencing reads have been submitted to the NCBI Sequence Read Archive (<https://www.ncbi.nlm.nih.gov/bioproject/PRJNA790633>). Other data and code have been made available in Supplementary Information and at Dryad (<https://doi.org/10.5061/dryad.b2rbnzsh2>), and are organized per figure.

Received: 7 July 2021; Accepted: 11 January 2022;

Published online: 03 March 2022

References

- de Visser, J. A. G. M. & Krug, J. Empirical fitness landscapes and the predictability of evolution. *Nat. Rev. Genet.* **15**, 480–490 (2014).
- Lässig, M., Mustonen, V. & Walczak, A. M. Predicting evolution. *Nat. Ecol. Evol.* **1**, 77 (2017).
- Mas, A., Lagadeuc, Y. & Vandenkoornhuys, P. Reflections on the predictability of evolution: toward a conceptual framework. *iScience* **23**, 101736 (2020).
- Palmer, A. C. & Kishony, R. Understanding, predicting and manipulating the genotypic evolution of antibiotic resistance. *Nat. Rev. Genet.* **14**, 243–248 (2013).
- Sommer, M. O. A. et al. Prediction of antibiotic resistance: time for a new preclinical paradigm? *Nat. Rev. Microbiol.* **15**, 689–696 (2017).
- Baym, M. et al. Spatiotemporal microbial evolution on antibiotic landscapes. *Science* **353**, 1147–1151 (2016).
- Good, B. H. et al. The dynamics of molecular evolution over 60,000 generations. *Nature* **551**, 45–50 (2017).
- Tenaillon, O. et al. The molecular diversity of adaptive convergence. *Science* **335**, 457–461 (2012).
- Sandegren, L. & Andersson, D. I. Bacterial gene amplification: implications for the evolution of antibiotic resistance. *Nat. Rev. Genet.* **7**, 578–588 (2009).
- Orr, H. A. The population genetics of beneficial mutations. *Phil. Trans. R. Soc. B* **365**, 1195–1201 (2010).
- Sniegowski, P. D. & Gerrish, P. J. Beneficial mutations and the dynamics of adaptation in asexual populations. *Phil. Trans. R. Soc. B* **365**, 1255–1263 (2010).
- Orr, H. A. The distribution of fitness effects among beneficial mutations. *Genetics* **163**, 1519–1526 (2003).
- Bailey, S. F. et al. What drives parallel evolution? *BioEssays* **39**, e201600176 (2017).
- Garoff, L. et al. Population bottlenecks strongly influence the evolutionary trajectory to fluoroquinolone resistance in *Escherichia coli*. *Mol. Biol. Evol.* **37**, 1637–1646 (2020).
- Storz, J. F. Causes of molecular convergence and parallelism in protein evolution. *Nat. Rev. Genet.* **17**, 239–250 (2016).
- Orr, H. A. The probability of parallel evolution. *Evolution* **59**, 216–220 (2005).
- Gerrish, P. J. & Lenski, R. E. The fate of competing beneficial mutations in an asexual population. *Genetica* **102**, 127–144 (1998).
- Good, B. H. et al. Distribution of fixed beneficial mutations and the rate of adaptation in asexual populations. *Proc. Natl Acad. Sci. USA* **109**, 4950–4955 (2012).
- Gomez, K., Bertram, J. & Masel, J. Mutation bias can shape adaptation in large asexual populations experiencing clonal interference. *Proc. R. Soc. B* **287**, 20201503 (2020).
- Payne, J. L. et al. Transition bias influences the evolution of antibiotic resistance in *Mycobacterium tuberculosis*. *PLoS Biol.* **17**, e3000265 (2019).
- Sackman, A. M. et al. Mutation-driven parallel evolution during viral adaptation. *Mol. Biol. Evol.* **34**, 3243–3253 (2017).
- Stoltzfus, A. & McCandlish, D. M. Mutational biases influence parallel adaptation. *Mol. Biol. Evol.* **34**, 2163–2172 (2017).
- Svensson, E. I. & Berger, D. The role of mutation bias in adaptive evolution. *Trends Ecol. Evol.* **34**, 422–434 (2019).
- MacLean, R. C., Perron, G. G. & Gardner, A. Diminishing returns from beneficial mutations and pervasive epistasis shape the fitness landscape for rifampicin resistance in *Pseudomonas aeruginosa*. *Genetics* **186**, 1345–1354 (2010).
- Storz, J. F. et al. The role of mutation bias in adaptive molecular evolution: insights from convergent changes in protein function. *Phil. Trans. R. Soc. B* **374**, 20180238 (2019).
- Ochs, I. E. & Desai, M. The competition between simple and complex evolutionary trajectories in asexual populations. *BMC Evol. Biol.* **15**, 55 (2015).
- Salverda, M. L. M. et al. Initial mutations direct alternative pathways of protein evolution. *PLoS Genet.* **7**, e1001321 (2011).
- Salverda, M. L. M. et al. Adaptive benefits from small mutation supplies in an antibiotic resistance enzyme. *Proc. Natl Acad. Sci. USA* **114**, 12773–12778 (2017).
- Szendro, I. G. et al. Predictability of evolution depends non-monotonically on population size. *Proc. Natl Acad. Sci. USA* **110**, 571–576 (2013).
- Windels, E. M. et al. Population bottlenecks strongly affect the evolutionary dynamics of antibiotic persistence. *Mol. Biol. Evol.* **38**, 3345–3357 (2021).
- Mahrt, N. et al. Bottleneck size and selection level reproducibly impact antibiotic resistance evolution. *Nat. Ecol. Evol.* **5**, 1233–1242 (2021).
- Woods, R. J. et al. Second-order selection for evolvability in a large *Escherichia coli* population. *Science* **331**, 1433–1436 (2011).
- Consuegra, J. et al. Insertion-sequence-mediated mutations both promote and constrain evolvability during a long-term experiment with bacteria. *Nat. Commun.* **12**, 980 (2021).
- de Visser, J. A. G. M. et al. Diminishing returns from mutation supply rate in asexual populations. *Science* **283**, 404–406 (1999).
- Rozen, D. E. et al. Heterogeneous adaptive trajectories of small populations on complex fitness landscapes. *PLoS ONE* **3**, e1715 (2008).
- Salverda, M. L. M., de Visser, J. A. G. M. & Barlow, M. Natural evolution of TEM-1 beta-lactamase: experimental reconstruction and clinical relevance. *FEMS Microbiol. Rev.* **34**, 1015–1036 (2010).
- Woods, R. et al. Tests of parallel molecular evolution in a long-term experiment with *Escherichia coli*. *Proc. Natl Acad. Sci. USA* **103**, 9107–9112 (2006).
- Kim, S. W. et al. Outer membrane vesicles from beta-lactam-resistant *Escherichia coli* enable the survival of beta-lactam-susceptible *E. coli* in the presence of beta-lactam antibiotics. *Sci. Rep.* **8**, 5402 (2018).
- Andersson, D. I. & Hughes, D. Gene amplification and adaptive evolution in bacteria. *Annu. Rev. Genet.* **43**, 167–195 (2009).
- Lind, P. A. et al. Predicting mutational routes to new adaptive phenotypes. *eLife* **8**, e38822 (2019).
- Maddamsetti, R. et al. Core genes evolve rapidly in the long-term evolution experiment with *Escherichia coli*. *Genome Biol. Evol.* **9**, 1072–1083 (2017).
- Eyre-Walker, A. & Keightley, P. D. The distribution of fitness effects of new mutations. *Nat. Rev. Genet.* **8**, 610–618 (2007).
- Sanjuán, R., Moya, A. & Elena, S. F. The distribution of fitness effects caused by single-nucleotide substitutions in an RNA virus. *Proc. Natl Acad. Sci. USA* **101**, 8396–8401 (2004).
- Schenk, M. F. et al. Quantifying the adaptive potential of an antibiotic resistance enzyme. *PLoS Genet.* **8**, e1002783 (2012).
- Blank, D. et al. The predictability of molecular evolution during functional innovation. *Proc. Natl Acad. Sci. USA* **111**, 3044–3049 (2014).
- Chavhan, Y., Malusare, S. & Dey, S. Larger bacterial populations evolve heavier fitness trade-offs and undergo greater ecological specialization. *Heredity* **124**, 726–736 (2020).
- Pinheiro, F. et al. Metabolic fitness landscapes predict the evolution of antibiotic resistance. *Nat. Ecol. Evol.* **5**, 677–687 (2021).
- Raesis, C. et al. Large chromosomal rearrangements during a long-term evolution experiment with *Escherichia coli*. *mBio* **5**, e01377-14 (2014).
- Lopatkin, A. J. et al. Clinically relevant mutations in core metabolic genes confer antibiotic resistance. *Science* **371**, eaba0862 (2021).
- Nicoloff, H. et al. The high prevalence of antibiotic heteroresistance in pathogenic bacteria is mainly caused by gene amplification. *Nat. Microbiol.* **4**, 504–514 (2019).
- Lachapelle, J., Reid, J. & Colegrave, N. Repeatability of adaptation in experimental populations of different sizes. *Proc. R. Soc. B* **282**, 20143033 (2015).
- van Dijk, T. et al. Mutation supply and the repeatability of selection for antibiotic resistance. *Phys. Biol.* **14**, 055005 (2017).
- Miller, C. R., Joyce, P. & Wichman, H. A. Mutational effects and population dynamics during viral adaptation challenge current models. *Genetics* **187**, 185–202 (2011).

54. Lenski, R. E. et al. Long-term experimental evolution in *Escherichia coli*. I. Adaptation and divergence during 2,000 generations. *Am. Nat.* **138**, 1315–1341 (1991).
55. Barlow, M. & Hall, B. G. Predicting evolutionary potential: in vitro evolution accurately reproduces natural evolution of the TEM beta-lactamase. *Genetics* **160**, 823–832 (2002).
56. Lewontin, R. C. The interaction of selection and linkage. I. General considerations; heterotic models. *Genetics* **49**, 49–67 (1964).

Acknowledgements

We thank B. Koopmanschap (deceased) for practical help, and D. Aanen, S.-C. Park, S. Das, M. Lässig and A. Stoltzfus for comments and discussion. This work was supported by DFG grant SFB680 to M.F.S., M.P.Z., S.H., J.K. and J.A.G.M.d.V.; DFG grant CRC1310 to J.K. and J.A.G.M.d.V.; HFSP Research Grant RGP0010/2015 to P.R. and J.A.G.M.d.V.; and an EMBO fellowship (ALTF 273-2017) to P.R. The funders had no role in study design, data collection and analysis, decision to publish or preparation of the manuscript.

Author contributions

M.F.S. and J.A.G.M.d.V. conceptualized the study; M.F.S., J.K. and J.A.G.M.d.V. designed the experiments; M.F.S., M.P.Z. and P.R. conducted the experiments; M.F.S., M.P.Z.,

S.H., P.R., E.S., J.K. and J.A.G.M.d.V. analysed the data; M.F.S., M.P.Z., P.R., J.K. and J.A.G.M.d.V. wrote the manuscript.

Competing interests

The authors declare no competing interests.

Additional information

Extended data is available for this paper at <https://doi.org/10.1038/s41559-022-01669-3>.

Supplementary information The online version contains supplementary material available at <https://doi.org/10.1038/s41559-022-01669-3>.

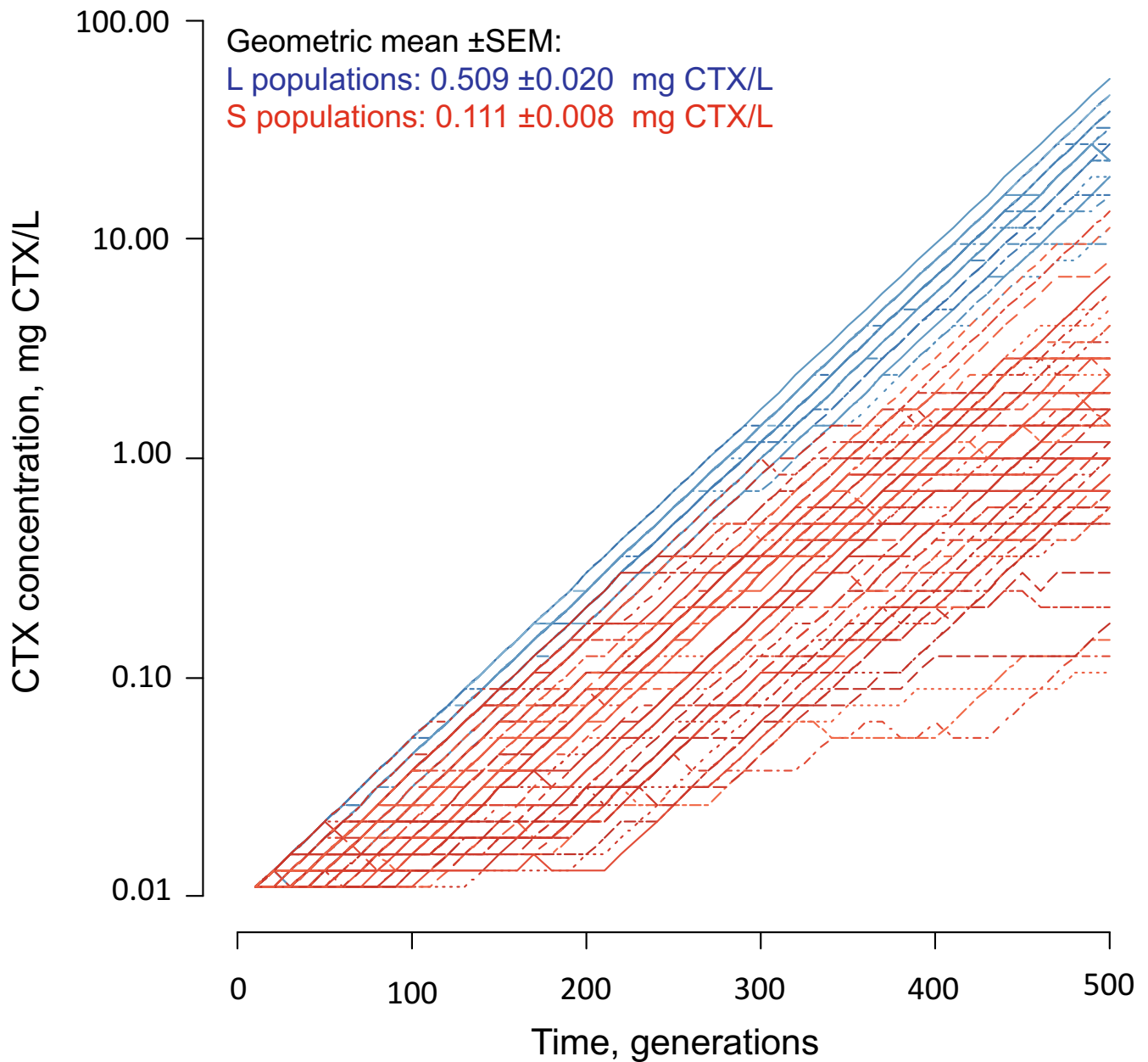
Correspondence and requests for materials should be addressed to Mark P. Zwart or J. Arjan G. M. de Visser.

Peer review information *Nature Ecology & Evolution* thanks Craig MacLean, Isabel Gordo and Philip Gerrish for their contribution to the peer review of this work. Peer reviewer reports are available.

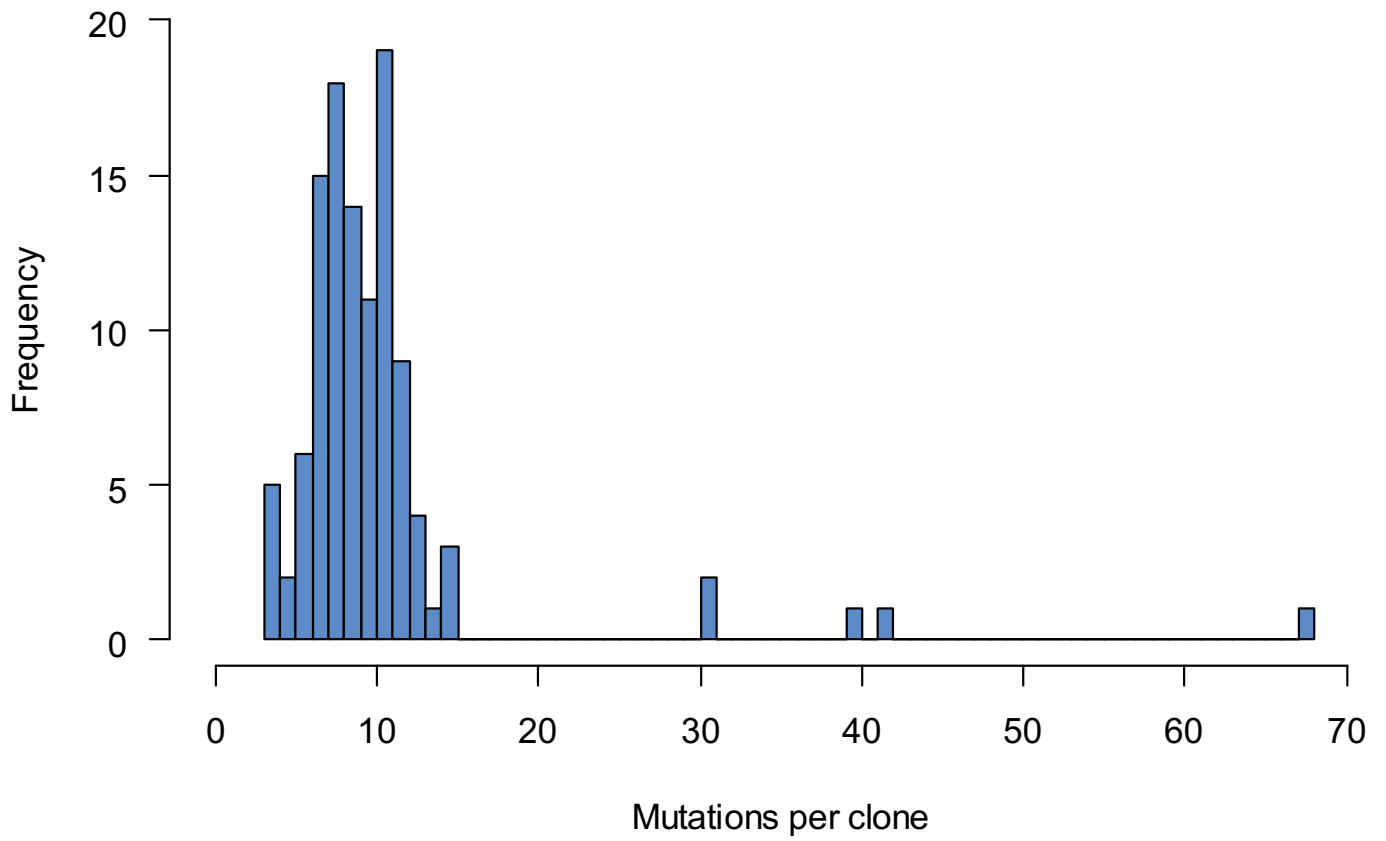
Reprints and permissions information is available at www.nature.com/reprints.

Publisher's note Springer Nature remains neutral with regard to jurisdictional claims in published maps and institutional affiliations.

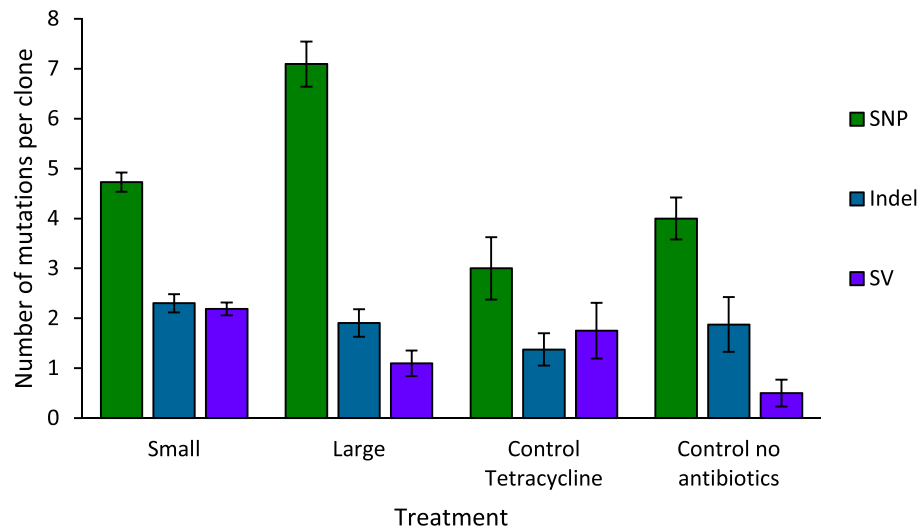
© The Author(s), under exclusive licence to Springer Nature Limited 2022



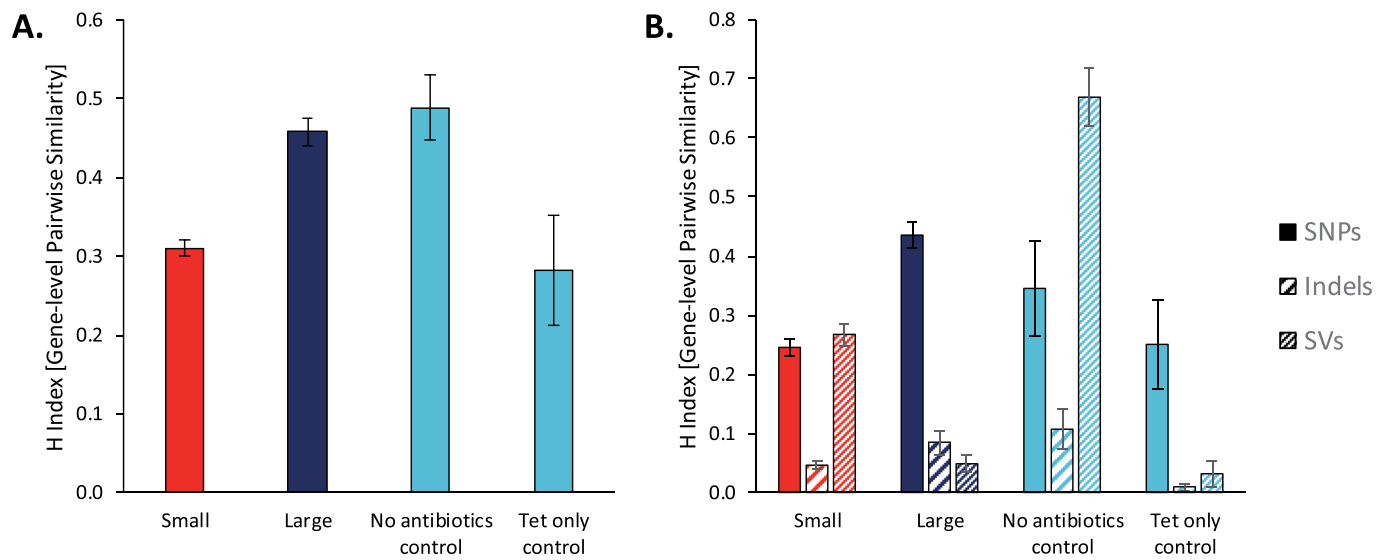
Extended Data Fig. 1 | CTX concentrations during the evolution experiment. CTX concentrations during the evolution experiment based on daily $2^{0.25}$ -fold increases when the OD_{600} was higher than 75% of the ancestral value without CTX (see text). Red lines represent small populations (S), blue lines large populations (L). Shades and line types have been varied randomly to better distinguish replicate populations. Note that for one large population the CTX concentration was increased during every round of passaging, as the cultures always reached a high density. For two other large populations, this was the case on all but one round of passaging.



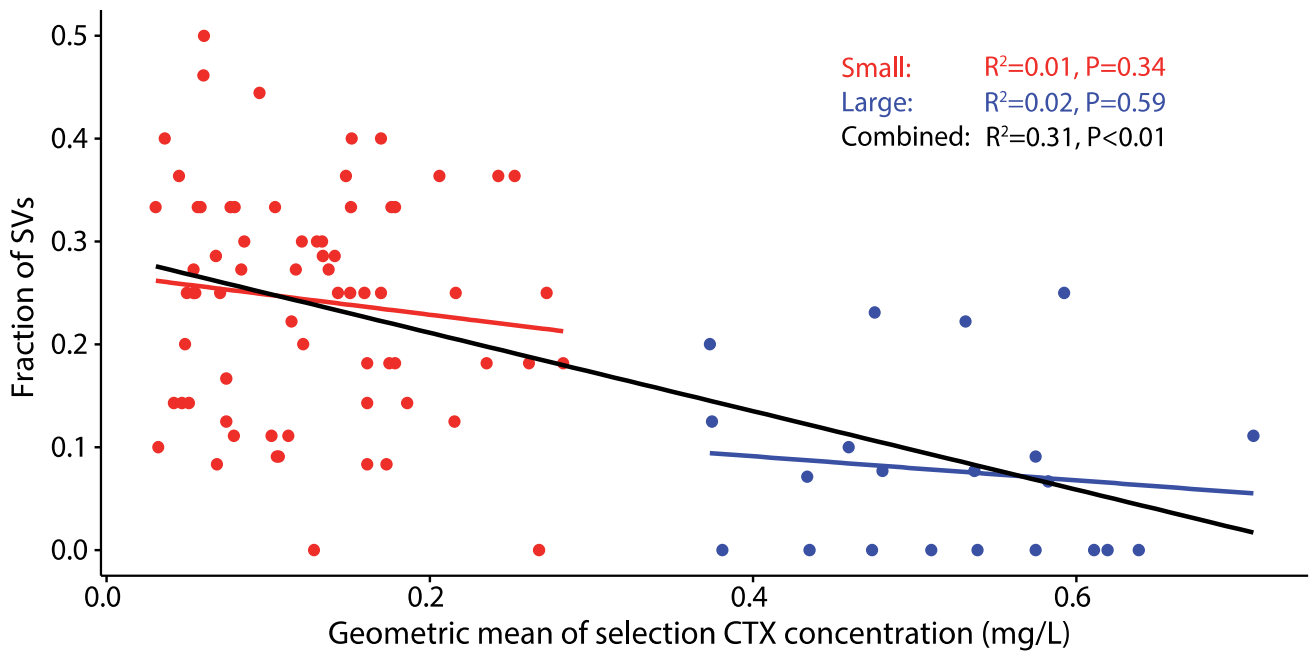
Extended Data Fig. 2 | Histogram of the number of mutations per clone. Histogram of the number of mutations per clone, for all 112 populations.



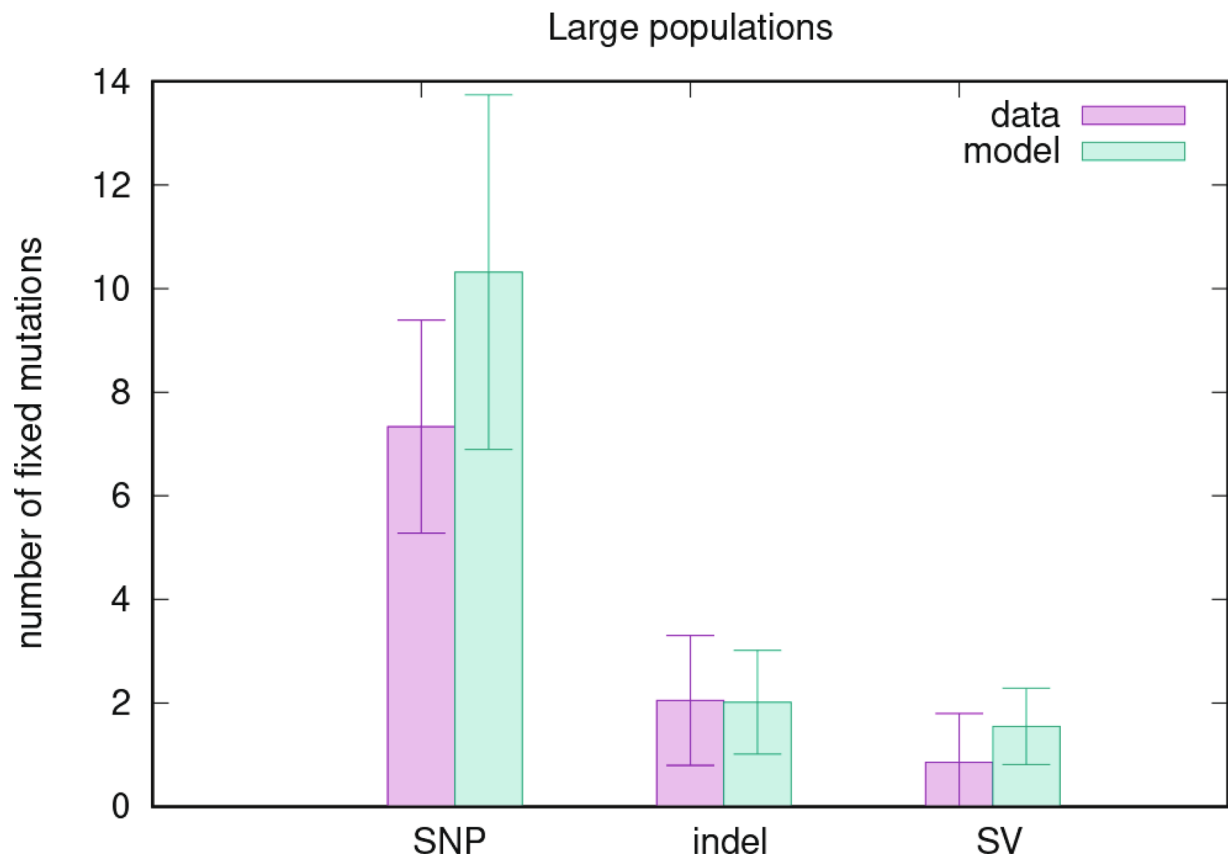
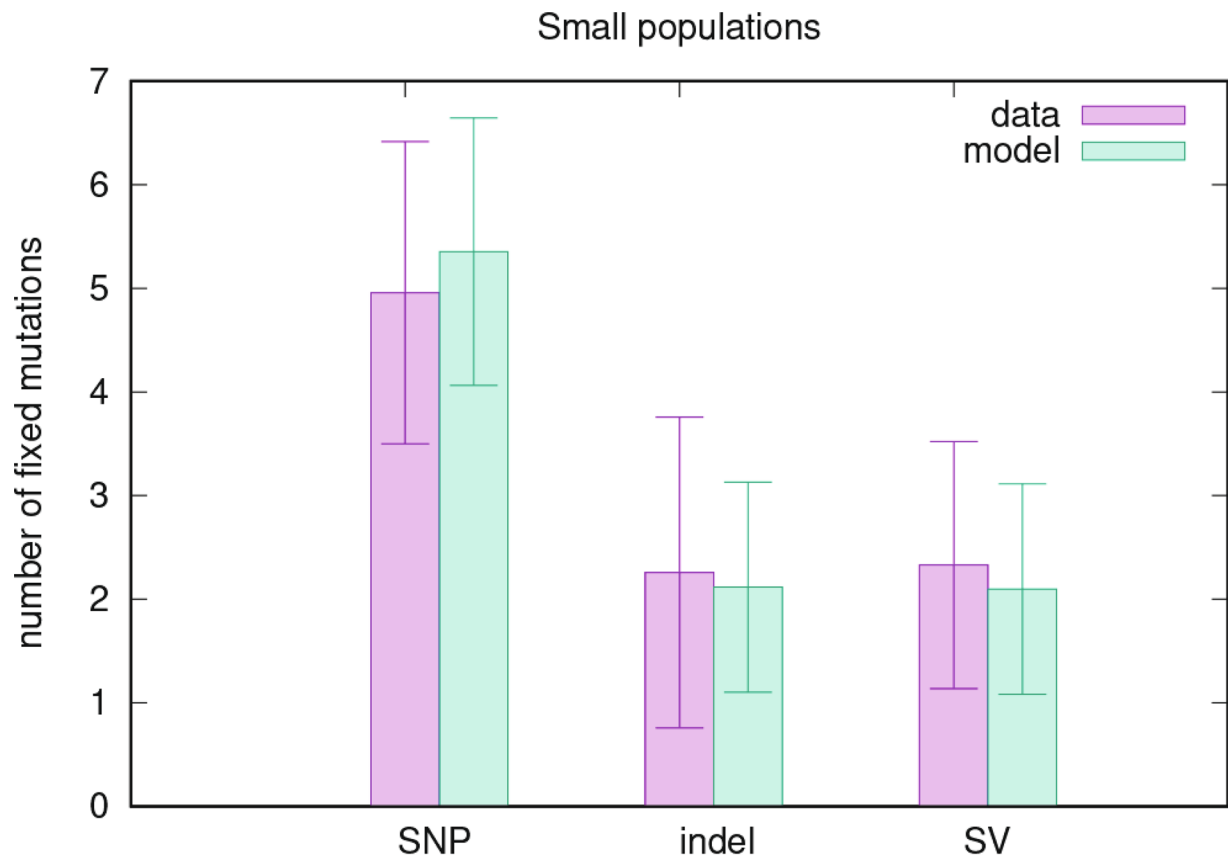
Extended Data Fig. 3 | Mutation frequency per mutation class and treatment. Mutation frequency per mutation class and per treatment for the 107 non-mutator populations. Error bars indicate the standard error of the mean. SNPs are green, Indels are blue, and SVs are purple. Error bars indicate the standard error of the mean.



Extended Data Fig. 4 | Gene-level H-indexes. (a) Gene-level *H*-index is given for all mutational events in clones from non-mutator populations. (b) Gene-level *H*-index is given for three classes of mutational events, as indicated by the legend.



Extended Data Fig. 5 | Regression analysis of the fraction of SVs against CTX concentration. Regression analysis of the fraction of SVs among all mutations per clone against CTX concentration.



Extended Data Fig. 6 | See next page for caption.

Extended Data Fig. 6 | Distribution of predicted and observed mutations in the final clones. Distribution of fixed mutations at the evolutionary endpoint obtained from the optimized WF model in comparison to the experimental data. Column heights represent the mean number of mutations and error bars show the corresponding standard deviation.

Reporting Summary

Nature Portfolio wishes to improve the reproducibility of the work that we publish. This form provides structure for consistency and transparency in reporting. For further information on Nature Portfolio policies, see our [Editorial Policies](#) and the [Editorial Policy Checklist](#).

Statistics

For all statistical analyses, confirm that the following items are present in the figure legend, table legend, main text, or Methods section.

n/a Confirmed

- The exact sample size (n) for each experimental group/condition, given as a discrete number and unit of measurement
- A statement on whether measurements were taken from distinct samples or whether the same sample was measured repeatedly
- The statistical test(s) used AND whether they are one- or two-sided
Only common tests should be described solely by name; describe more complex techniques in the Methods section.
- A description of all covariates tested
- A description of any assumptions or corrections, such as tests of normality and adjustment for multiple comparisons
- A full description of the statistical parameters including central tendency (e.g. means) or other basic estimates (e.g. regression coefficient) AND variation (e.g. standard deviation) or associated estimates of uncertainty (e.g. confidence intervals)
- For null hypothesis testing, the test statistic (e.g. F , t , r) with confidence intervals, effect sizes, degrees of freedom and P value noted
Give P values as exact values whenever suitable.
- For Bayesian analysis, information on the choice of priors and Markov chain Monte Carlo settings
- For hierarchical and complex designs, identification of the appropriate level for tests and full reporting of outcomes
- Estimates of effect sizes (e.g. Cohen's d , Pearson's r), indicating how they were calculated

Our web collection on [statistics for biologists](#) contains articles on many of the points above.

Software and code

Policy information about [availability of computer code](#)

Data collection

Wallac version [Kun je dit aanvullen, Arjan? Philip weet dit waarschijnlijk wel.] for the Perkin Elmer Victor³ plate reader, and the Cologne Center for Genomics performed high-throughput sequencing analysis on Illumina platforms with Illumina Software.

Data analysis

All software used for analysis is also described in the Methods Section and Supplementary Materials. CLC Genomics Workbench version 8.01 (Qiagen Bioinformatics) was used for analysis of sequencing data. Data analysis was primarily performed in R 3.6.1 (The R Foundation, Vienna). Relevant code has been included in the overview of data files, together with primary data.

For manuscripts utilizing custom algorithms or software that are central to the research but not yet described in published literature, software must be made available to editors and reviewers. We strongly encourage code deposition in a community repository (e.g. GitHub). See the Nature Portfolio [guidelines for submitting code & software](#) for further information.

Data

Policy information about [availability of data](#)

All manuscripts must include a [data availability statement](#). This statement should provide the following information, where applicable:

- Accession codes, unique identifiers, or web links for publicly available datasets
- A description of any restrictions on data availability
- For clinical datasets or third party data, please ensure that the statement adheres to our [policy](#)

Accession codes for reference sequences used are provided in the supplementary materials (REL606 genome: Genbank NC_012967.1, pACTEM1 plasmid: Genbank MN386081). There are no restrictions on data availability. Sequencing data has been submitted to the NCBI Sequence Read Archive under BioProject PRJNA790633. Other data and code have been made available in the Supplementary Information file and at Dryad (doi:10.5061/dryad.b2rbnzsh2), and are organized per figure.

Field-specific reporting

Please select the one below that is the best fit for your research. If you are not sure, read the appropriate sections before making your selection.

Life sciences Behavioural & social sciences Ecological, evolutionary & environmental sciences

For a reference copy of the document with all sections, see [nature.com/documents/nr-reporting-summary-flat.pdf](https://www.nature.com/documents/nr-reporting-summary-flat.pdf)

Ecological, evolutionary & environmental sciences study design

All studies must disclose on these points even when the disclosure is negative.

Study description	Fifty serial passages were performed with four treatments: small population size with increasing novel antibiotic (72 independent replicates), large population size with increasing novel antibiotic (24 independent replicates), and 2 control conditions (only an antibiotic to select for plasmid maintenance, and no antibiotics at all; 8 replicates each). Characterization of the evolved populations was based on a randomly selected clone, but complemented were possible with analyses on the evolved populations to show these clones were representative for the evolved populations. For all analyses of evolved clones, at least three biological replicates (i.e., independent preculturing of the clone prior to any experiment) were performed.
Research sample	Two near-identical, well characterized laboratory strains were used and transformed with a previously characterized plasmid. Our research is basic work about evolutionary dynamics, and therefore our research sample is not intended to be representative of any real-world population.
Sampling strategy	No sample size calculations were performed, as the study is exploratory. We did choose a high level of replication because the study focuses on the repeatability of evolution.
Data collection	Serial passage experiments, DNA extractions and preparation for sequencing, and MIC measurements were performed by Martijn Schenk and technician Bertha Koopmanschap. Library preparation and high-throughput sequencing were performed by the Cologne Center for Genomics, as a service. Measurements of beta-lactamase activity and the fitness of selected mutants were performed by Philip Ruelens.
Timing and spatial scale	NA.
Data exclusions	No data were excluded from the analyses.
Reproducibility	For the serial passaging, we have specified in the supplementary materials problems that occurred and how we dealt with them: "On three occasions, growth in control wells with medium was detected. In those cases, the entire plate was restarted from the previous day's plate, which was stored at 4C. On two occasions the wrong Ara-marker type was detected in a small population, and those populations were restarted from frozen samples from the previous time point." For subsequent analyses of the evolved populations, all experiments were deemed to be executed successfully and were included in the analyses.
Randomization	Clones for initiating each replicate in the experiment were picked from an agar plate of bacteria transformed with the pACTEM plasmid.
Blinding	There was no blinding. Key observations for decisions that needed to be made here in the experiment and subsequent analysis are based on simple quantitative measurements. For example, optical density 600 values were measured on cultures to determine whether antibiotic concentrations would be increased or to determine whether populations grew during antibiotic resistance measurements.

Did the study involve field work? Yes No

Reporting for specific materials, systems and methods

We require information from authors about some types of materials, experimental systems and methods used in many studies. Here, indicate whether each material, system or method listed is relevant to your study. If you are not sure if a list item applies to your research, read the appropriate section before selecting a response.

Materials & experimental systems

n/a	Involved in the study
<input checked="" type="checkbox"/>	<input type="checkbox"/> Antibodies
<input checked="" type="checkbox"/>	<input type="checkbox"/> Eukaryotic cell lines
<input checked="" type="checkbox"/>	<input type="checkbox"/> Palaeontology and archaeology
<input checked="" type="checkbox"/>	<input type="checkbox"/> Animals and other organisms
<input checked="" type="checkbox"/>	<input type="checkbox"/> Human research participants
<input checked="" type="checkbox"/>	<input type="checkbox"/> Clinical data
<input checked="" type="checkbox"/>	<input type="checkbox"/> Dual use research of concern

Methods

n/a	Involved in the study
<input checked="" type="checkbox"/>	<input type="checkbox"/> ChIP-seq
<input checked="" type="checkbox"/>	<input type="checkbox"/> Flow cytometry
<input checked="" type="checkbox"/>	<input type="checkbox"/> MRI-based neuroimaging